Ocean climate variability and travel surveillance data inform understanding of global dengue dynamics

Stella Dafka[1,2*], Kristina M. Angelo[3], Rhett J. Stoney[3], Kevin O'Laughlin[3], Alexandre Duvignaud[4,5], Michael Libman[6], Davidson H. Hamer[7-9], Joacim Rocklöv[1,2], Ralph Huits[10]

1 Heidelberg Institute of Global Health, Faculty of Medicine, Heidelberg University, Heidelberg, Germany

2 Interdisciplinary Center for Scientific Computing, Faculty of Mathematics and Computer Science, Heidelberg University, Heidelberg, Germany

3 Division of Global Migration Health, Centers for Disease Control and Prevention, Atlanta, GA, USA

4 Department of Infectious Diseases and Tropical Medicine, Division of Tropical Medicine and Clinical International Health, Hôpital Pellegrin, CHU Bordeaux, Bordeaux, France

5 Global Health in the Global South - University of Bordeaux, National Institute for Health and Medical Research (INSERM) UMR 1219 - Research Institute for Sustainable Development (IRD) EMR 271, Bordeaux Population Health Research Centre, Bordeaux, France

6 J.D. MacLean Centre for Tropical Diseases, McGill University, Montreal, Canada

7 Department of Global Health, Boston University School of Public Health, Boston, MA, USA

8 Section of Infectious Disease, Department of Medicine, Boston University Chobanian & Avedisian School of Medicine, Boston, MA, USA

9 Center on Emerging Infectious Diseases, Boston University, Boston, MA, USA

10 Department of Infectious Tropical Diseases and Microbiology, IRCCS Sacro Cuore Don Calabria Hospital, Negrar, Verona, Italy

Corresponding author: Stella Dafka
E-mail: stella.dafka@uni-heidelberg.de

Abstract

Oceanic-atmospheric interactions significantly influence regional rainfall and vector-borne disease dynamics. Travel-related dengue cases serve as effective sentinels for dengue transmission, yet the impact of sea surface temperature (SST) variability on their occurrence remains under explored. Here we analyzed 2000–2019 GeoSentinel traveler dengue data alongside ERA5 SST and precipitation anomalies to assess correlations across global ocean basins. We identified that dominant SST variability modes in the Indian, Pacific, and Atlantic Oceans are remotely associated with dengue incidence in regions exhibiting strong seasonal precipitation patterns. These SST-driven rainfall variations likely modulate vector ecology and dengue transmission. Incorporating SST and precipitation anomalies into dengue forecasting models could enhance outbreak prediction and public health preparedness, providing a valuable adjunct to existing tools.

Introduction

Anthropogenic climate change is triggering cascading effects that pose unprecedented threats to human health (1). Among these, vector-borne infections such as West Nile, Dengue, Chikungunya, and Zika viruses are particularly climate-sensitive, with global warming altering their spatial and temporal distribution, transmission pathways, and epidemiology (2-6). The increasing environmental suitability for vector activity has been identified as a key indicator of the negative impacts of climate change on human health (7), and without effective control efforts, the burden of these diseases is projected to rise substantially by 2100 (4).

Dengue is a major global public health threat in more than 120 tropical and sub-tropical countries (8), many of which are popular travel destinations. As a result of vector habitat expansion, 22% more countries on all continents will have weather conditions conducive to dengue transmission by the end of this century (9). While the influence of many local climate variables such as temperature, precipitation, and relative humidity on dengue transmission dynamics has been extensively studied in many regions (10), the roles of remote climate drivers —large-scale climate phenomena originating far from the affected regions— in the occurrence and predictability of dengue outbreaks have received less attention (11). For example, Lowe et al. (12) demonstrated the potential of climate forecasts and statistical models to predict the 2016 dengue season in Machala, Ecuador, using climate forecasts and statistical models, highlighting the value of climate services in outbreak management. Petrova et al. (13) found that only strong El Niño events can lead to earlier-than-expected occurrence of dengue outbreaks.

Components of the climate system with long-term memory, such as sea surface temperatures (SSTs), can potentially predict regional hydroclimate (14). SST anomalies (SSTA) influence atmospheric circulation and moisture, with warmer SSTs increasing evaporation and atmospheric water vapor, which in turn leads to higher rainfall (15, 16). SSTA are major precursors of tropical precipitation variability (17, 18), playing a significant role in modulating dominant modes of variability such as the El Niño–Southern Oscillation (ENSO) and the Indian Ocean Dipole (IOD). Numerous studies confirm that regional hydroclimatic conditions can drive vector-borne disease outbreaks, as excessive precipitation, drought, and elevated temperatures increase vulnerability to infectious diseases through complex cascading risk pathways (19). SST thus offers a potential source of predictability with longer lead times (20) and could be leveraged to provide early-warning signals for disease transmission and dengue epidemiology (11).

Infected returning international travelers not only contribute to the importation and spread of dengue in non-endemic subregions, but can also serve as sentinels (early indicators) of dengue circulation at their travel destinations (21-23).

Accordingly, we evaluated the effectiveness of GeoSentinel data (24) in detecting dengue outbreaks by validating its signal against large external datasets. We further examined the relationship between travel-related dengue cases and oceanic SST variability and total precipitation (TP), to identify potential large-scale circulation drivers by subregion and season. Our aim is to incorporate these features into future dengue forecasting models as an adjunct to existing outbreak prediction tools.

Materials and Methods

Dengue cases

GeoSentinel is a global sentinel surveillance and research network of the US Centers for Disease Control and Prevention and the International Society of Travel Medicine that monitors travel-associated health hazards (25, 26). Demographics, travel history, and clinical data from international travelers are entered into the GeoSentinel database (Appendix) by clinicians at 70 travel and tropical medicine sites in 29 countries. We retrieved all confirmed and probable dengue cases of returned travelers from 2000–2019 that had sufficient data available to ascertain the timing and country of dengue exposure. The travel end date (TED) was used as a proxy for the date of illness onset. We validated the GeoSentinel signaling strength as sentinel for dengue transmission in the subregions defined by the Intergovernmental Panel on Climate Change (IPCC, Appendix Fig S1A) against dengue case counts by year and country from the Global Infectious Disease and Epidemiology Online Network (GIDEON; 27), a dynamic database that records trends in global infectious diseases. We assessed the strength of association between the GeoSentinel and GIDEON datasets using parametric (Pearson productmoment correlation) and non-parametric (Spearman test) tests, at a significance level of alpha ≤ 0.05 for either test.

Climate variables

Hourly estimates of SST and TP from 2000–2019 were retrieved from the latest generation of European Centre for Medium-Range Weather Forecasts global atmospheric reanalysis, ERA5 (28), with a horizontal resolution of 0.25°. ERA5 provides an accurate representation of the SST spatiotemporal variability (29), it captures the locations and patterns of precipitation totals (30) and exhibits lower precipitation biases and errors than its predecessor ERA-interim (31).

Spatial Pattern Analysis

We investigated the lag structures and the associated spatial distribution patterns of correlation coefficients between GeoSentinel's dengue cases and SSTA and TP over the IPCC subregions that exhibit distinct monsoon characteristics and strong seasonality in precipitation (Appendix Fig S1-S2), including Central America and Mexico, South America, sub-Saharan Africa, South Asia, and Southeast Asia (Fig 1). The daily mean SSTs were computed from hourly estimates. The hourly accumulated precipitation fields were summed to form the 24-hour precipitation totals. Then, for both variables, daily anomalies were calculated as the differences from the climatological mean over the study period (2000–2019), which was smoothed using a 5-day running mean. Weekly mean values were calculated from the daily values for both ERA5 fields and aggregated at each subregion across the study period.

Fig 1. Geographical subregions of dengue exposure along with the number of travel related dengue cases (%), GeoSentinel, 2000-2019. Country codes are according to the international standard ISO 3166.

Spatial distribution patterns of correlation coefficients between the number of travel-related dengue cases with averaged SSTA and TP over the period 2000–2019 were derived at different timeframes. For each ERA5 grid point, time series of travel-related dengue from the same subregion were correlated with time series of SSTA and TP to assess statistical dependence (32) between SSTA and TP and travel-related dengue. SSTA and TP fields were averaged over a 7-day window for the country of dengue exposure, considering 1, 8, 12 and 24 weeks prior to the TED (hereafter x-week lag). This approach allowed us to assess the consistency of the spatial distribution patterns associated with dengue cases and to identify potential large-scale climatic signals at various lead times. Considering up to 24-week lagged climate patterns enabled exploration of the predictive potential of SST variability modes at sub-seasonal to seasonal scales. Each week was assigned to a season depending on the subregion (Table 1), accounting for pronounced differences of climatic conditions. Although outbreaks have traditionally occurred during the wet season when vector abundance increases, recent climate variability and change have disrupted established patterns of disease seasonality (33), so all seasons were considered where data were available. Statistical significance ($p \leq 0.05$) was assessed via two-tailed t-test. To evaluate the link between SSTA, TPA and the travel-related dengue, we computed composites of SSTA and TPA at time lags of up to 24 weeks for each season (Appendix Fig S3-S7). Fig 2 provides a schematic overview of the applied method. To assess the impact of the choice of reference period (2000–2019), anomalies have also been computed using the 30-year baseline, 1991–2020 (34). Similar patterns and signals were identified in both reference periods, indicating that the reference interval does not affect the results and or their interpretation.

Table 1. Seasons analyzed by subregion, including the regional monsoon system that is typically affected.

Subregion	Seasons	Regional monsoon system
Central America and Mexico	wet: May-October dry: November-April	North American monsoon

South America	pre-monsoon: September-November monsoon: December-February post-monsoon: March-May dry: June-August	South American monsoon
Sub-Saharan Africa	EA monsoon: March-May WA monsoon: June-September	East and West African monsoons
South Asia	pre-monsoon: March-May monsoon: June-September post-monsoon: October-November dry: December-February	Indian summer monsoon
Southeast Asia	wet: May-October dry: November-April	Southeast Asia monsoon

Fig 2. Schematic overview of the analytical approach. Sea surface temperature anomalies (SSTA) and total precipitation (TP) are correlated (r) with travel-related dengue cases at multiple time lags preceding the travel end date (TED). Lag −i represents the i-th week before TED (Lag −1, −8, −16, and −24).

Results

Dengue cases

We included 5,275 records of travelers with dengue acquired in 95 countries and who were evaluated at 66 GeoSentinel network sites. Dengue cases were clustered by IPCC subregion, based on the country of acquisition (Fig 1). Approximately 52% of cases (N=2,765) reported recent travel to Southeast Asia (Fig 1). The GeoSentinel and GIDEON datasets were found to be significantly correlated ($p \leq 0.05$) in all subregions except the Caribbean (Appendix Table 1), suggesting that the GeoSentinel dengue cases are valid sentinels of dengue transmission in five out of six subregions under study.

Spatial Pattern Analysis

We report the results of the spatial patterns of correlation coefficients between the travel-related dengue and SSTA and TP per season (Table 1) and subregion (Fig 1), for the 24-, 12-, 8- and 1-week lags before the TED (Fig 3-7). To assess the relationship between SSTA and TPA and travel-related dengue, we investigate the spatial structure and magnitude of the SST and TP anomaly fields using a composite analysis (Appendix Fig S3-S7).

Central America and Mexico

In both seasons, positive correlations were found between travel-related dengue acquired in Central America and Mexico, and SSTAs over the subtropical and tropical North Pacific and Atlantic oceans in all lag weeks (Fig 3a-d). In the dry season, a tripole pattern emerged, characterised by positive correlations off the east coast of the United States and negative correlations north of 50°N and south of 20°N (more pronounced in the dry season; Fig 3c,d). Additionally, during the dry season, persistent positive correlations were observed over the eastern equatorial Pacific (Fig 3c, d). The signal to the east is consistent with the SST pattern being closely linked to North Atlantic Oscillation (NAO) variability (35), and that to the west is similar to the ENSO. Both signals were strongest at 16- and 24-week lags and confirmed by the SSTA composite maps (Appendix Fig S3c,d).

Travel-related dengue was positively associated with TP in both seasons, especially along the Pacific coasts of Mexico and Central America (Fig 3e-h). The signal is more pronounced 1- and 8-week lags before the TED and diminishes afterwards (at 16- and 24-week lags). This is also evident in the composite TPA anomaly patterns (Fig S3e-h) where wetter-than-average conditions have been identified in both seasons (more pronounced in the wet season) across the central and eastern equatorial Pacific, which are typically associated with El Niño. Positive precipitation anomalies over land have only been identified up to two months before the TED (1- and 8-week lags; Fig S3e-h).

Fig 3. Spatial pattern of correlation coefficients in Central America and Mexico. (a-d) Spatial distribution maps of correlation coefficients between sea surface temperature anomalies (SSTA) and (e-h) total precipitation (TP) with travel-related dengue cases at (a,c,e,g) lag of 8 (Lag-8) and (b,d,f,h) 1 week (Lag-1) before the travel end date for (a,b,e,f) wet (May-October) and (c,d,g,h) dry (November-April) seasons in Central America and Mexico for 2000–2019. Red (blue) shades indicate positive (negative) correlation between SSTA and travel-related dengue cases. The opposite applies for TP. Stippling denotes statistically significant areas at the 95% level.

South America

In the pre-monsoon season, positive correlations were identified between SSTA and travel-related dengue off the western coast of Central America and the Caribbean Sea, as well as in the central equatorial Atlantic, at 1- and 8-week lags (Fig 4a,b). During the monsoon and post-monsoon seasons, statistically significant positive correlations were observed in the equatorial Pacific, with the strongest signal at the 24-week lag (Fig 4c,d,f). The monsoon SSTA composites resembled the distinct El Niño pattern (Appendix Fig S4c-f). In the post-monsoon season, positive correlations were also observed in the southern Pacific Ocean (~20°S), accompanied by negative correlations further south (~30–40°S), except for the 8-week lag (Fig 4e). This pattern is spatially consistent with the South Pacific Meridional Mode (SPMM; 36), a dominant air-sea coupling mode in the subtropical southeastern Pacific (Appendix Fig S4f). During the dry season, strong positive correlations between travel-related dengue and SSTA were found in the subtropical and tropical North Atlantic Ocean, most pronounced at 8-, 16-, and 24-week lags (Fig 4g,h), consistent with the SSTA composite maps (Appendix Fig S4g,h).

We found positive correlations between TP and travel-related dengue in the pre-monsoon, monsoon, and post-monsoon seasons over the entire South American region except for northeastern Brazil, at 1-week lag (Fig 4j,l,n). The signal ceases in the pre-monsoon period (Fig 4i) and diminishes during the monsoon and post-monsoon periods, but is still evident up to 8- and 16-week lag (Fig 4k,m). In the dry period, positive correlations between travel-related dengue and TP comprised a broad area extending across northern South America and northeastern Brazil evident up to 8-week lag (Fig 4o,p). TPA patterns have been observed to resemble those typically associated with El Niño in the Pacific Ocean and Atlantic Niño in the Atlantic Ocean (Fig 4i-p). These patterns are evident in all weeks during the monsoon and post-monsoon seasons, and are most pronounced at 16- and 24-week lags during the pre-monsoon and dry seasons.

Fig 4. Spatial pattern of correlation coefficients in South America. (a-h) Spatial distribution maps of correlation coefficients between sea surface temperature anomalies (SSTA) and (i-p) total precipitation (TP) with travel-related dengue cases at (a,c,e,g and i,k,m,o) lag of 8 (Lag-8) and (b,d,f,h and j,l,n,p) 1 week (Lag-1) before the travel end date in (a,b,i,j) pre-monsoon (September-November), (c,d,k,l) monsoon (December-February), (e,f,m,n) post-monsoon (March-May), and (g,h,o,p) dry season (June-August) in South America for 2000–2019. Red (blue) shades indicate positive (negative) correlation between SSTA and travel-related dengue cases. The opposite applies for TP. Stippling denotes statistically significant areas at the 95% level.

Sub-Saharan Africa

During the East African (EA) monsoon season, we identified positive correlations between travel-related dengue acquired in sub-Saharan Africa and SSTA in the south-eastern tropical Atlantic Ocean (20–30°S) and the western tropical Indian Ocean off Madagascar (30°S), accompanied by negative anomalies west of Australia (most intense at an 8-week lag; Fig 5a). Similar and stronger patterns were identified during the West African (WA) monsoon season, while the signal over the southeastern tropical Atlantic shifted northwards (between 10°S and 20°S; Fig 5c,d). These signals are also visible in the SSTA composites (see Appendix Fig S5a–d), indicating the relative influence of the Mascarene high region and the southern tropical Atlantic SSTs on dengue cases in Africa.

Spatial patterns of correlation coefficients for TP followed the seasonal rainfall variability of the sub-Saharan African subregions, showing positive correlation coefficients between travel-related dengue with rainfall south of the equator in EA monsoon season (Fig 5e,f), and north of the equator in WA monsoon season (Fig 5g,h), consistent with the TPA composite patters (Appendix Fig S5e-h).

Fig 5. Spatial pattern of correlation coefficients in sub-Saharan Africa. (a-d) Spatial distribution maps of correlation coefficients between sea surface temperature anomalies (SSTA) and (e-h) total precipitation (TP) with travel-related dengue cases at (a,c) lag of 8 (Lag-8) and (b,d,f,h) 1 week (Lag-1) before the travel end date for (a,b,e,f) EA monsoon (March-May) and (c,d,g,h) WA monsoon (June-September) seasons in sub-Saharan Africa for 2000–2019. Red (blue) shades indicate positive (negative) correlation between SSTA and travel-related dengue cases. The opposite applies for TP. Stippling denotes statistically significant areas at the 95% level.

South Asia

The number of travel-related dengue from South Asia was positively associated with SSTA extending over the South Indian Ocean and negatively associated with SSTA extending over the eastern Indian Ocean, west of Sumatra (Fig 6a-f). This was evident in all seasons except the dry season (Fig 6g,h) and was most pronounced during the monsoon and post-monsoon seasons (Fig 6c-f). This signal is spatially consistent with the positive IOD pattern, a prominent mode of climate variability in the tropical Indian Ocean (37), which is also apparent in the composite maps (Appendix Fig 6a-f). Additionally, significant positive correlations were observed between travel-related dengue and SSTA in the equatorial Pacific in all seasons except the post-monsoon season (Fig 6a–h). This pattern is most evident in the pre-monsoon and dry seasons, 8–16-weeks before TED, and in the monsoon season, 24 weeks before TED. This signal displays a distinctive SST signature of El Niño that is also evident in the SSTA composite maps (Appendix Fig S6a-h). In addition, there was a positive correlation between travel-related dengue and SSTA over the subtropical South Indian Ocean (Fig 6a–h). This signal, which is most prevalent during the monsoon and dry seasons (see Fig 6c,d,g,h), displays a distinctive SST warming signature centred over the Mascarene High region (Appendix Fig S6a–h). Finally, travel-related dengue was positively correlated with SSTA over large parts of the Bay of Bengal and the Arabian Sea in the post-monsoon season (Fig 6e,f), and over the South China Sea in the dry season (Fig 6g,h).

The pre-monsoon precipitation signal was positive and intense over the east coast of India (evident up to the 16-week lag; Fig 6i,j), signifying the onset of convective activity and the transitional stage of the Indian summer monsoon. During the monsoon, a spatially coherent pattern was identified, characterized by significant positive associations between the travel-related dengue and rainfall across the domain evident up to the 16-week lag (Fig 6k,l). In post-monsoon, significant positive correlations extend spatially over most of the subregion, except central India (Fig 6m,n) and this was evident at 1-week lag. In the dry season, there was a significant positive correlation between travel-related dengue and TP in the northern parts of the Indian Peninsula, over the great Himalayan range, the western Himalayan, in north Pakistan and Nepal and in the southern part of India at the 1-week lag (Fig 6o,p). Total precipitation anomalies exhibit distinct patterns that are typically associated with the IOD, with an increase in rainfall in the western Indian Ocean and a decrease in the eastern region (Appendix Fig S6i-p). Positive equatorial precipitation anomalies are also evident (Appendix Fig S6i-p), indicating the signal of El Niño.

Fig 6. Spatial pattern of correlation coefficients in South Asia. (a-h) Spatial distribution maps of correlation coefficients between sea surface temperature anomalies (SSTA) and (i-p) total precipitation (TP) with travel-related dengue cases at (a,c,e,g and i,k,m,o) lag of 8 (Lag-8) and (b,d,f,h and j,l,n,p) 1 week (Lag-1) before the travel end date in (a,b,i,j) pre-monsoon (March-May), (c,d,k,l) monsoon (June-September), (e,f,m,n) post monsoon (October-November), and (g,h,o,p) dry season (December-February) in South Asia for 2000–2019. Red (blue) shades indicate positive (negative) correlation between SSTA and travel-related dengue cases. The opposite applies for TP. Stippling denotes statistically significant areas at the 95% level.

Southeast Asia

In both seasons, significant positive correlations between travel-related dengue from Southeast Asia and SSTA appeared over the South Indian Ocean between 10°N–20°S and in the South China Sea in all lag weeks (Fig 7a-d, most pronounce in the dry season). In the dry season, significant negative correlations have been identified over the Philippine Sea, in all lag weeks (Fig 7c,d). In addition, strong positive correlations have been identified over the equatorial Pacific (Fig 7a-d, most pronounce in the dry season), evident in all lag weeks in the dry season and at 16- and 24-week lags during the wet season. In the dry season, the western signal resembles the Indian Ocean Basin Mode (IOBM), while in the wet season it coincides with the Mascarene High region. Meanwhile, the eastern signal indicates the emerge of El Niño during the dry season. These signals are evident in the SSTA composites (Appendix Fig S7a–d).

The pattern of correlation coefficients between travel-related dengue and TP revealed a clear dipole in Southeast Asia. In the wet season, significant positive correlations peaked over the Philippines and the western portion of the Indochina Peninsula (Fig 7e,f), while in the dry season, significant positive correlations were observed over the eastern portion of the Indochina Peninsula and the Maritime Continent (Fig 7g,h). TPA patterns were consistent, displaying both this distinct dipole across seasons and lag weeks, as well as the El Niño signal, which was most prominent in the dry season (Appendix Fig S7i-l).

Fig 7. Spatial pattern of correlation coefficients in Southeast Asia. (a-d) Spatial distribution maps of correlation coefficients between sea surface temperature anomalies (SSTA) and (e-h) total precipitation (TP) with travel-related dengue cases at (a,c,e,g) lag of 8 (Lag-8) and (b,d,f,h) 1 week (Lag-1) before the travel end date for (a,b,e,f) wet (May- October) and (c,d,g,h) dry (November-April) seasons in Southeast Asia for 2000–2019. Red (blue) shades indicate positive (negative) correlation between SSTA and travel-related dengue cases. The opposite applies for TP. Stippling denotes statistically significant areas at the 95% level.

Discussion

This analysis provides new insights into how surges in travel-related dengue cases respond to oceanic SST anomalies (SSTAs) and total precipitation (TP), revealing that these surges are influenced by coherent spatial SST structures across the global oceans. Large-scale SST features in the Indian, Pacific, and Atlantic Oceans could be incorporated into future dengue forecasting models as an adjunct to existing outbreak prediction tools.

Our analysis suggests that, when compared with the GIDEON database, the 2000–2019 GeoSentinel dataset of returning international travelers with dengue was significantly correlated with dengue transmission in all subregions, except the Caribbean. Sentinel surveillance of health hazards in returning international such as that routinely conducted by GeoSentinel, plays a pivotal role in the detection of travel-associated infections, and it may identify outbreaks in countries or territories with limited local public health surveillance capacity (25). Over the past decades, GeoSentinel has identified and reported multiple outbreaks of vector-borne diseases, including Zika in Costa Rica (38, 39), chikungunya in Myanmar (40-42), and yellow fever in Brazil (Hamer et al. 2018). GeoSentinel data has the potential to complement public health surveillance by local authorities, which is the prime source for data collection by GIDEON. Failure to detect cases can contribute to the unnoticed spread of the disease (43).

Our findings demonstrate the existence of co-varying relationships between the numbers of travel-related dengue cases acquired in the geographic regions of dengue exposure and SSTA in the Pacific, Atlantic, and Indian Oceans and TP. They highlight the importance of understanding the coupling between oceanic SSTA and precipitation. The findings also suggest that combining climatological data with epidemiological observations may help inform the development of early-warning systems for regional occurrence of dengue outbreaks.

The spatial distribution maps of the correlation coefficients between travel-related dengue and SSTA show considerable seasonal variation. The strongest correlations are observed at 16- and 24-week lags in subregions associated with dominant large-scale modes of climate variability, as summarized in Fig 8. For TP, stronger correlations are found at 1- and 8- week lags in subregions with higher monsoon precipitation rates, reflecting the influence of seasonal rainfall regimes driven by monsoon variability. Overall, coherent spatial SST structures in the oceans are correlated with rainfall variability, which may be associated with mosquito population dynamics and vector biology, and thus may affect the risk of dengue incidence in each subregion.

Fig 8. Potential (non-exclusive) sea surface temperature–related climate drivers of travel-related dengue by subregion and month. Subregions are shown along the x-axis: Central America (CAM), South America (SAM), South Asia (SAS), Southeast Asia (SEA), and Sub-Saharan Africa (SSA). Climate drivers (secondary y-axis) include El Niño, Subtropical North Pacific (SNP), Subtropical North Atlantic (SNA), Caribbean Sea (CAR), North Atlantic Oscillation (NAO), South Pacific Meridional Mode (SPMM), Central Equatorial Atlantic (CEA), Mascarene High region (MH), Subtropical Atlantic (STA), Indian Ocean Dipole (IOD), Indian Ocean Basin Mode (IOBM), Arabian Sea (AS), Bay of Bengal (BOB), and South China Sea (SCS).

In Central America, a clear relationship was found between SSTAs and travel-related dengue over the north-eastern and eastern equatorial Pacific oceans, as well as the subtropical North Atlantic. Previous studies have examined the associations between Central America's precipitation and Pacific/Atlantic SSTs (44-46). The NAO and the El Niño are strongly correlated with dengue cases. The NAO has been found to be a driver of Mesoamerican monsoon variability (47), while Central America's and Mexico's winter precipitation tend to be strongly associated to ENSO (46). In South America, travel-related dengue is correlated with the Atlantic and Pacific SSTs. The strongest associations are with the El Niño, the SPMM and the SSTAs in the subtropical and tropical north Atlantic. El Niño has been linked to precipitation anomalies in South America (48), while the SPMM has been shown to trigger the onset of ENSO (36, 49). Ciemer et al. (50) investigated the relationship between SST and rainfall anomalies using a complex network approach and found that rainfall sums in the Amazon Basin are mainly affected by SSTA in the southern Pacific Ocean. In sub-Saharan Africa, travel-related dengue is correlated with SST patterns in the Mascarene High region and the South tropical Atlantic Ocean. Previous studies have demonstrated the importance of both regions for wet conditions and rainfall variability in sub-Saharan Africa (51, 52). In South Asia, travel-related dengue is correlated with the positive IOD and El Niño patterns as well as SSTA over the subtropical southern Indian Ocean. Persistent subtropical warm SSTA over this region induces positive IOD events through modulation of the Mascarene High (53). The role of the southern Indian Ocean circulation in the Indian summer monsoon is well established, while oscillations in the strength of the Mascarene High are linked to variability in monsoon rainfall and SSTs over the Indian Ocean (54-56). The IOD pattern has been found to be strongly correlated with the Indian summer monsoon rainfall (57). In Southeast Asia, travel-related dengue is correlated with the IOBM and El Niño patterns. The IOBM is associated with a uniform warming across the basin, which may have led to enhanced convection, resulting in wetter conditions over the maritime continent, promoting vectorial capacity. Finally, El Niño has been linked to the amplification of endemic diseases, such as dengue, in South and Southeast Asia (58, 59).

Our study has several limitations. Although GeoSentinel surveillance data include a large number of cases, they represent a convenience sample and are subject to biases related to patient referral patterns, data recording and reporting by designated sites, and fluctuations in travel volumes. Therefore, even though dengue frequencies recorded by GeoSentinel correlated with the GIDEON database for all subregions, the data are not fully generalizable. While subregions were delineated based on physical processes important to regional climatology, such as strong seasonality of precipitation, the observed SSTA and TPA signals are sensitive to the spatial extent of these subregions. Analyses of correlations between SSTA and TP fields and dengue cases identify empirical linkages and statistical dependencies, but do not establish causal relationships.

The interaction between climate and travel-related dengue is complex and dynamic. Advanced statistical methods using longer timeseries and climate indices are required to further elucidate the role of the ocean-atmospheric coupling on SST and regional TP patterns, that may predict dengue outbreaks. Advanced understanding of the driving mechanisms of monsoon precipitation is needed to better anticipate weather extremes, such as droughts and floods and devise prevention measures against dengue outbreaks.

Ethics statement

The GeoSentinel data collection protocol was reviewed by a human subjects advisor at CDC's National Center for Emerging and Zoonotic Infectious Diseases (NCEZID) and was determined to be public health surveillance and not human subjects research. Additional ethical clearance was obtained as required by the participating institutions. Informed consent was not required.

Funding

GeoSentinel, the Global Surveillance Network of the International Society of Travel Medicine (ISTM), is supported by a Cooperative Agreement (1 U01 CK000632-04) from the Centers for Disease Control and Prevention (CDC), as well as funding from the ISTM and the Public Health Agency of Canada. The analysis was co-funded by the GeoSentinel Foundation and Alexander von Humboldt Foundation.

Disclaimer

The findings and conclusions in this report are those of the authors and do not necessarily represent the official position of the US Centers for Disease Control and Prevention.

Data statement

The dengue case data supporting the results of this study are available from the authors upon reasonable request and with permission from the GeoSentinel Surveillance Network. The climate data analyzed in this study are available in the Copernicus Climate Data Store repository at https://cds.climate.copernicus.eu/.

Acknowledgments

We thank the GeoSentinel Surveillance Network and its participating sites for providing access to travel-related dengue surveillance data and for their continued contributions to global infectious disease monitoring. We also acknowledge the European Centre for Medium-Range Weather Forecasts (ECMWF) and the Copernicus Climate Change Service for providing the ERA5 reanalysis data used in this study.

References

1. IPCC. Climate Change 2022: Impacts, Adaptation, and Vulnerability. Contribution of Working Group II to the Sixth Assessment Report of the Intergovernmental Panel on Climate Change. Cambridge: Cambridge University Press; 2022. doi:10.1017/9781009325844.

2. Rocklöv J, Dubrow R. Climate change: an enduring challenge for vector-borne disease prevention and control. Nat Immunol. 2020;21:479–483.

3. Semenza JC, Rocklöv J, Penttinen P, Lindgren E. Observed and projected drivers of emerging infectious diseases in Europe. Ann N Y Acad Sci. 2016;1382(1):73–83.

4. Mora C, McKenzie T, Gaw IM, et al. Over half of known human pathogenic diseases can be aggravated by climate change. Nat Clim Chang. 2022;12(9):869–875.

5. Baylis M, Risley C. Climate change effects on infectious diseases. In: Shulman LM, ed. Infectious Diseases. Encyclopedia of Sustainability Science and Technology. New York: Springer; 2012.

6. McIntyre KM, Setzkorn C, Hepworth PJ, et al. Systematic assessment of the climate sensitivity of important human and domestic animal pathogens in Europe. Sci Rep. 2017;7:7134.

7. van Daalen KR, Tonne C, Semenza JC, et al. The 2024 Europe report of the Lancet Countdown on health and climate change. Lancet Public Health. 2024;9(7):e495–e522.

8. World Health Organization. Weekly epidemiological record – Dengue situation report. Geneva: WHO; 2025. Available from: https://www.who.int/publications/i/item/who-wer10052-665-678

9. McKinnon M, Lissner T, Romanello M, et al. Climate Vulnerability Monitor 2022: A Planet on Fire. Geneva: CVF & V20; 2022.

10. Soneja S, Tsarouchi G, Lumbroso D, et al. A review of dengue's historical and future health risk from a changing climate. Curr Environ Health Rep. 2021;8:245–265.

11. Chen Y, Xu Y, Wang L, et al. Indian Ocean temperature anomalies predict long-term global dengue trends. Science. 2024;384(6696):639–646.

12. Lowe R, Stewart-Ibarra AM, Petrova D, et al. Climate services for health: predicting the evolution of the 2016 dengue season in Machala, Ecuador. Lancet Planet Health. 2017;1(4):e142–e151.

13. Petrova D, Rodó X, Sippy R, et al. The 2018–2019 weak El Niño: predicting the risk of a dengue outbreak in Machala, Ecuador. Int J Climatol. 2021;41(7):3813–3823.

14. Sengupta A, Waliser DE, DeFlorio MJ, et al. Role of evolving sea surface temperature modes of variability in improving seasonal precipitation forecasts. Commun Earth Environ. 2025;6:256.

15. Cabrera M, Pezzi L, Santini M, Mendes C. Quantifying the influence of sea surface temperature anomalies on the atmosphere and precipitation in the southwestern Atlantic Ocean and southeastern South America. Atmosphere. 2025;16(7):887.

16. Good P, Chadwick R, Holloway CE, et al. High sensitivity of tropical precipitation to local sea surface temperature. Nature. 2021;589:408–414.

17. Liu T, Schmitt R, Li L. Global search for autumn-lead sea surface salinity predictors of winter precipitation in southwestern United States. Geophys Res Lett. 2018;45:8445–8454.

18. Mamalakis A, Yu JY, Randerson JT, et al. A new interhemispheric teleconnection increases predictability of winter precipitation in southwestern US. Nat Commun. 2018;9:4722.

19. Semenza JC, Rocklöv J, Ebi KL. Climate change and cascading risks from infectious disease. Infect Dis Ther. 2022;11(4):1371–1390.

20. Martineau P, Behera SK, Nonaka M, et al. Predicting malaria outbreaks from sea surface temperature variability up to 9 months ahead in Limpopo, South Africa. Front Public Health. 2022;10:962377.

21. Brem J, Elankeswaran B, Erne D, et al. Dengue homegrown in Europe, 2022–2023. New Microbes New Infect. 2023;56:101205.

22. Wong LP, Rajandra A, Abd Jamil J, et al. Effectiveness of dengue awareness calendar on indigenous populations. Healthcare (Basel). 2023;11(5):637.

23. Gossner CM, Fournet N, Frank C, et al. Dengue virus infections among European travellers, 2015–2019. Euro Surveill. 2022;27(2):2001937.

24. Duvignaud A, Stoney RJ, Angelo KM, et al. Epidemiology of travel-associated dengue from 2007 to 2022. J Travel Med. 2024;31(7):taae089.

25. Hamer DH, Rizwan A, Freedman DO, et al. GeoSentinel: past, present and future. J Travel Med. 2020;27(8):taaa219.

26. Huits R, Angelo KM, Amatya B, et al. Clinical characteristics and outcomes among travelers with severe dengue. Ann Intern Med. 2023;176:940–948.

27. Edberg SC. Global Infectious Diseases and Epidemiology Network (GIDEON). Clin Infect Dis. 2005;40(1):123–126.

28. Hersbach H, Bell B, Berrisford P, et al. ERA5 hourly data on single levels from 1940 to present. Copernicus Climate Change Service; 2023.

29. Yang C, et al. Sea surface temperature intercomparison in the framework of C3S. J Climate. 2021;34:5257–5283.

30. Lavers DA, Simmons A, Vamborg F, Rodwell MJ. Evaluation of ERA5 precipitation for climate monitoring. Q J R Meteorol Soc. 2022;148(748):3124–3137.

31. Nogueira M. Inter-comparison of ERA5, ERA-Interim and GPCP rainfall over the last 40 years. J Hydrol. 2020;583:124632.

32. Tjøstheim D, Otneim H, Støve B. Statistical dependence: beyond Pearson's rho. Stat Sci. 2022;37(1):90–109.

33. Baker RE, Mahmud AS, Miller IF, et al. Infectious disease in an era of global change. Nat Rev Microbiol. 2022;20:193–205.

34. Kawale J, Chatterjee SB, Kumar A, et al. Anomaly construction in climate data: issues and challenges. Proc CIDU. 2011:189–203.

35. Tian B, Fan K. Why is the North Atlantic Oscillation more predictable in December? Atmosphere. 2019;10:477.

36. Zhang H, Clement A, DiNezio P. The South Pacific meridional mode: a mechanism for ENSO-like variability. J Climate. 2014;27:769–783.

37. Saji N, Goswami B, Vinayachandran P, et al. A dipole mode in the tropical Indian Ocean. Nature. 1999;401:360–363.

38. Seers T, Rothe C, Hamer DH, et al. Zika virus infection in European travellers returning from Thailand in 2022. Trop Med Int Health. 2023;28(7):576–579.

39. Hamer DH, Barbre KA, Chen LH, et al. Travel-associated Zika virus disease acquired in the Americas through February 2016. Ann Intern Med. 2017;166.

40. Díaz-Menéndez M, Trigo EE, Ujiie M, et al. Travel-associated chikungunya acquired in Myanmar in 2019. Euro Surveill. 2020;25(1):1900721.

41. Dudouet P, Gautret P, Larsen CS, et al. Chikungunya resurgence in the Maldives and risk for importation to Europe. Travel Med Infect Dis. 2020;36:101814.

42. Javelle E, Florescu SA, Asgeirsson H, et al. Increased risk of chikungunya infection in travellers to Thailand, early 2019. Euro Surveill. 2019;24(10):1900146.

43. Hamer DH, Angelo K, Caumes E, et al. Fatal yellow fever in travelers to Brazil, 2018. MMWR Morb Mortal Wkly Rep. 2018;67(11):340–341.

44. Wright KT, et al. Precipitation in northeast Mexico controlled by Atlantic SST warming. Geophys Res Lett. 2022;49(11).

45. Martinez C, Goddard L, Kushnir Y, Ting M. Seasonal climatology and rainfall mechanisms in the Caribbean. Clim Dyn. 2019.

46. Pan Y, Zeng N, Mariotti A, et al. Covariability of Central America/Mexico winter precipitation and tropical SSTs. Clim Dyn. 2018;50:4335–4346.

47. Lachniet MS, Asmerom Y, Polyak V, Bernal JP. Two millennia of Mesoamerican monsoon variability. Quat Sci Rev. 2017;155:100–113.

48. Cai W, McPhaden MJ, Grimm AM, et al. Climate impacts of ENSO on South America. Nat Rev Earth Environ. 2020;1:215–231.

49. Zhang Z, Ren B, Zheng J. Leading modes of tropical Pacific subsurface ocean temperature. Sci Rep. 2017;7:42371.

50. Ciemer C, Rehm L, Kurths J, et al. Early-warning indicator for Amazon droughts based on tropical Atlantic SSTs. Environ Res Lett. 2020;15:094087.

51. Dyer E, Hirons L, Taye MT. July–September rainfall in the Greater Horn of Africa. Clim Dyn. 2022;59:3621–3641.

52. Frank LO, Sarthi PP. Causal relationships between monsoon systems and rainfall variability over Botswana. J Atmos Sci Res. 2024;7(3):129–146.

53. Feng J, Hu D, Yu L. Indian Ocean subtropical dipole and Mascarene high interactions. Acta Oceanol Sin. 2014;33:64–76.

54. Zhao Y, Wen Z, Li X, et al. Meridional variation of the Mascarene High. J Climate. 2023;36(19):6937–6950.

55. Morioka Y, Takaya K, Behera SK, et al. Local SST impacts on Mascarene High variability. J Climate. 2015;28(2):678–694.

56. Sarthi PP, Dash SK, Mamgain A. Changes in Indian summer monsoon under warmer climate. Glob Planet Change. 2012;92:17–29.

57. Ratna SB, Cherchi A, Osborn TJ, et al. Extreme positive Indian Ocean Dipole of 2019. Geophys Res Lett. 2021.

58. Anyamba A, Chretien JP, Britch SC, et al. Global disease outbreaks associated with the 2015–2016 El Niño event. Sci Rep. 2019;9:1930.

59. Mokhtar S, Pittman Ratterree DC, Britt AF, et al. Global risk of dengue outbreaks and impact of El Niño events. Environ Res. 2024;262:119830.

Author contributions

S.D., K.A., and R.H. wrote the manuscript. S.D., J.R., and R.H. designed the study. S.D. and R.S. performed data acquisition and cleaning. S.D. analyzed and interpreted the data. J.R. and R.H. supervised the study, and all authors discussed the results and commented on the manuscript and contributed with review and editing.

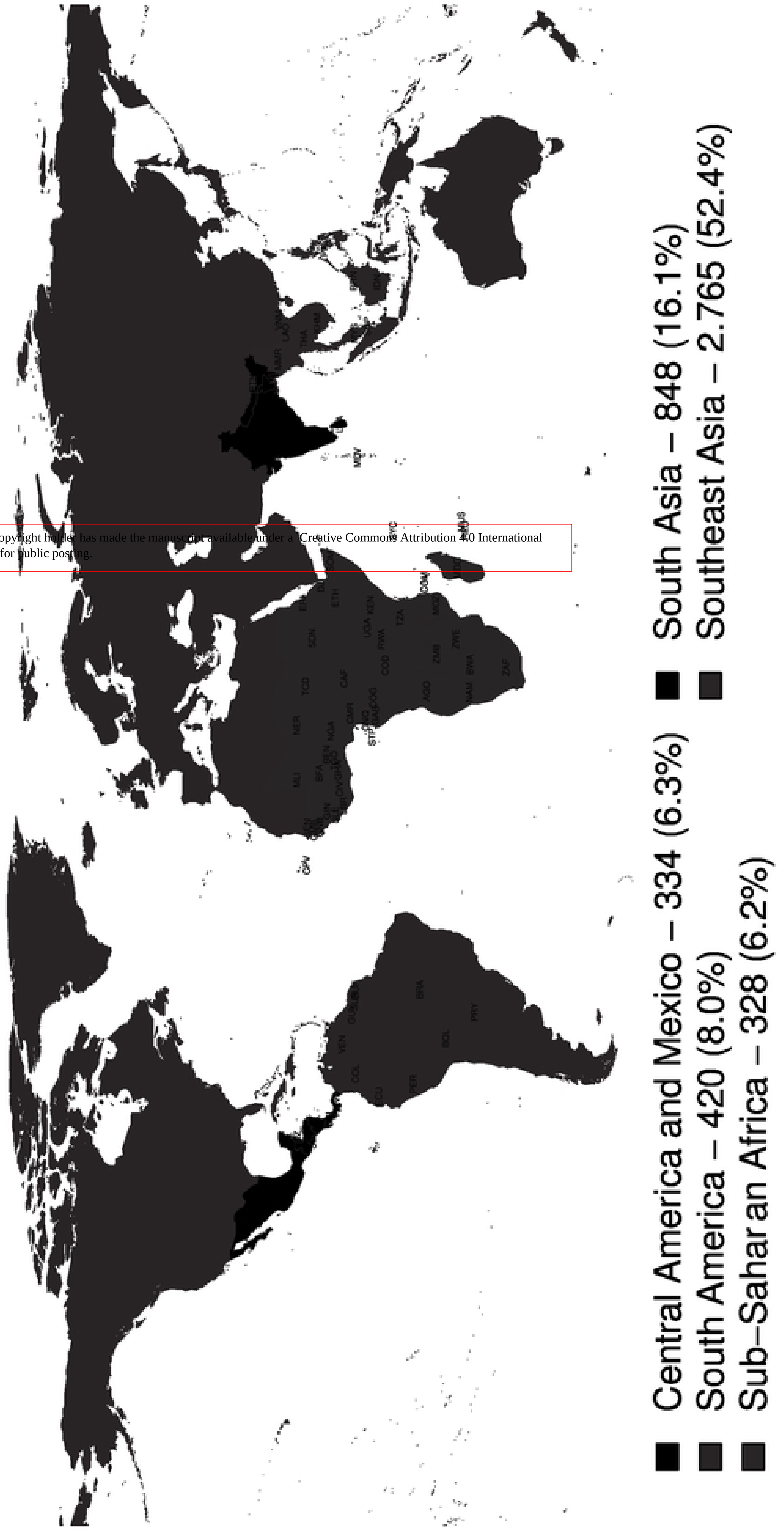
Central America and Mexico – 334 (6.3%)
South America – 420 (8.0%)
Sub–Saharan Africa – 328 (6.2%)
South Asia – 848 (16.1%)
Southeast Asia – 2.765 (52.4%)

Figure 1

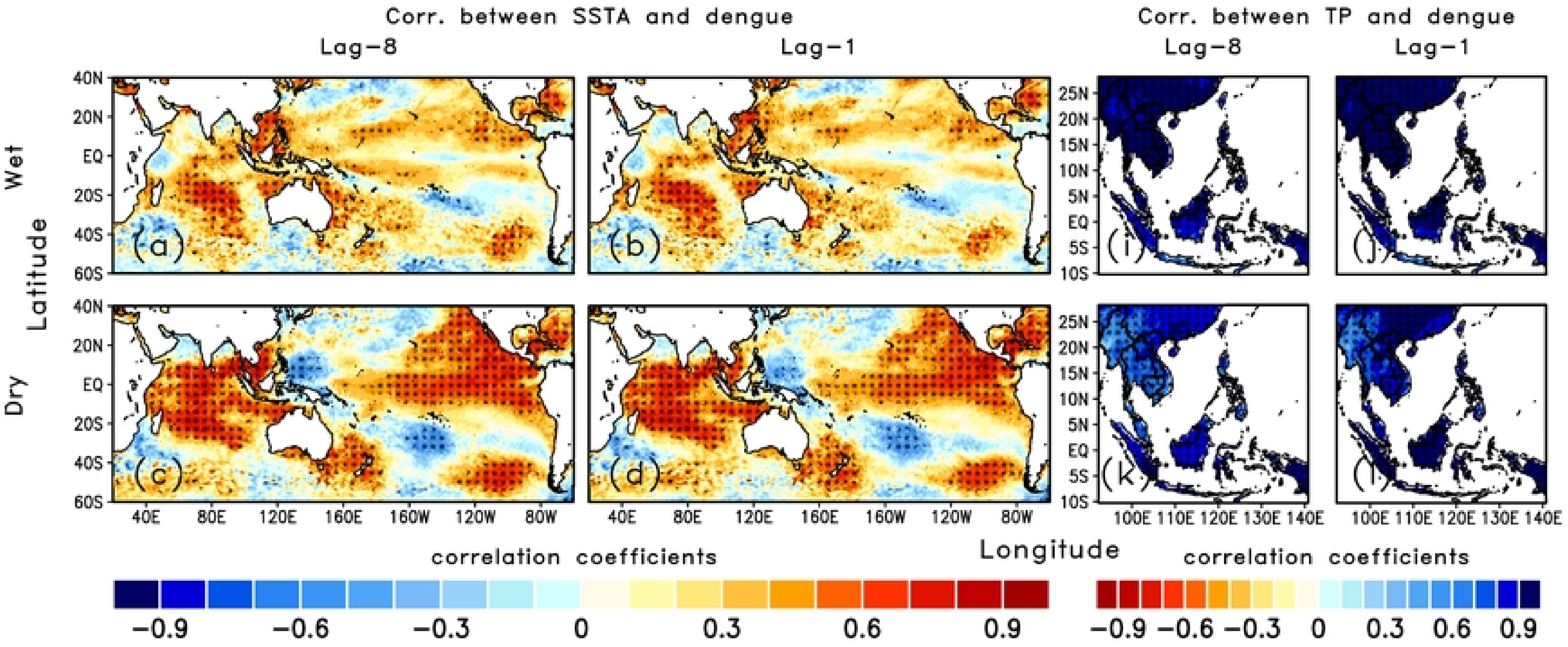
Corr. between SSTA and dengue
Lag-8
Lag-1
Corr. between TP and dengue
Lag-8
Lag-1
Wet
Dry
Latitude
Longitude
(a)
(b)
(c)
(d)
(i)
(j)
(k)
(l)
40N
20N
EQ
20S
40S
60S
25N
15N
10N
5N
5S
10S
40E
80E
120E
160E
160W
120W
80W
100E
110E
130E
140E
correlation coefficients
−0.9
−0.6
−0.3
0
0.3
0.6
0.9

Figure 7

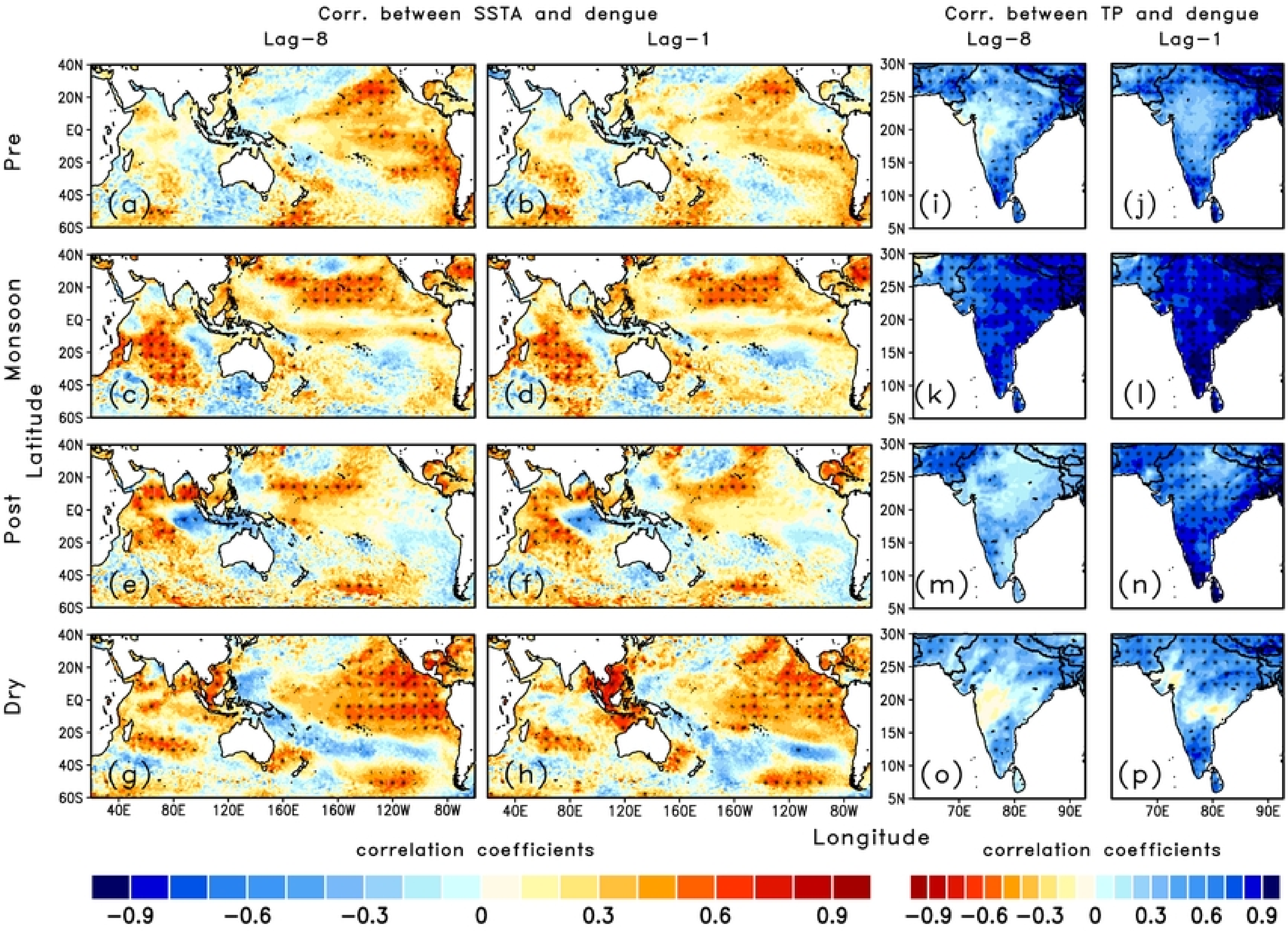

Corr. between SSTA and dengue
Lag-8
Lag-1
Corr. between TP and dengue
Lag-8
Lag-1
Pre
Monsoon
Post
Dry
Latitude
40N
20N
EQ
20S
40S
60S
30N
25N
20N
15N
10N
5N
(a)
(b)
(c)
(d)
(e)
(f)
(g)
(h)
(i)
(j)
(k)
(l)
(m)
(n)
(o)
(p)
40E
80E
120E
160E
160W
120W
80W
70E
80E
90E
Longitude
correlation coefficients
−0.9
−0.6
−0.3
0
0.3
0.6
0.9
correlation coefficients
−0.9
−0.6
−0.3
0
0.3
0.6
0.9

Figure 6

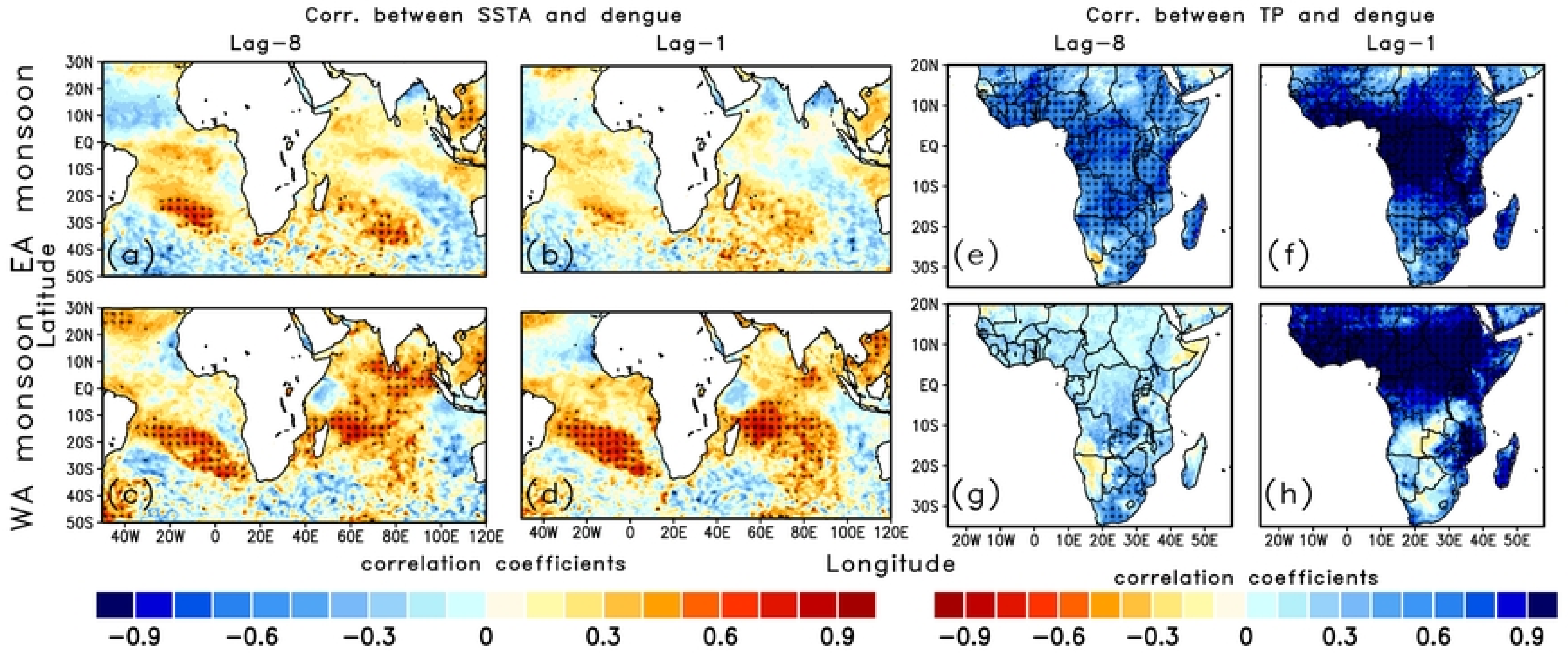
Corr. between SSTA and dengue
Corr. between TP and dengue
Lag-8
Lag-1
Lag-8
Lag-1
EA monsoon
WA monsoon
Latitude
Longitude
(a)
(b)
(c)
(d)
(e)
(f)
(g)
(h)
30N
20N
10N
EQ
10S
20S
30S
40S
50S
40W 20W 0 20E 40E 60E 80E 100E 120E
20W 10W 0 10E 20E 30E 40E 50E
correlation coefficients
−0.9 −0.6 −0.3 0 0.3 0.6 0.9
correlation coefficients
−0.9 −0.6 −0.3 0 0.3 0.6 0.9

Figure 5

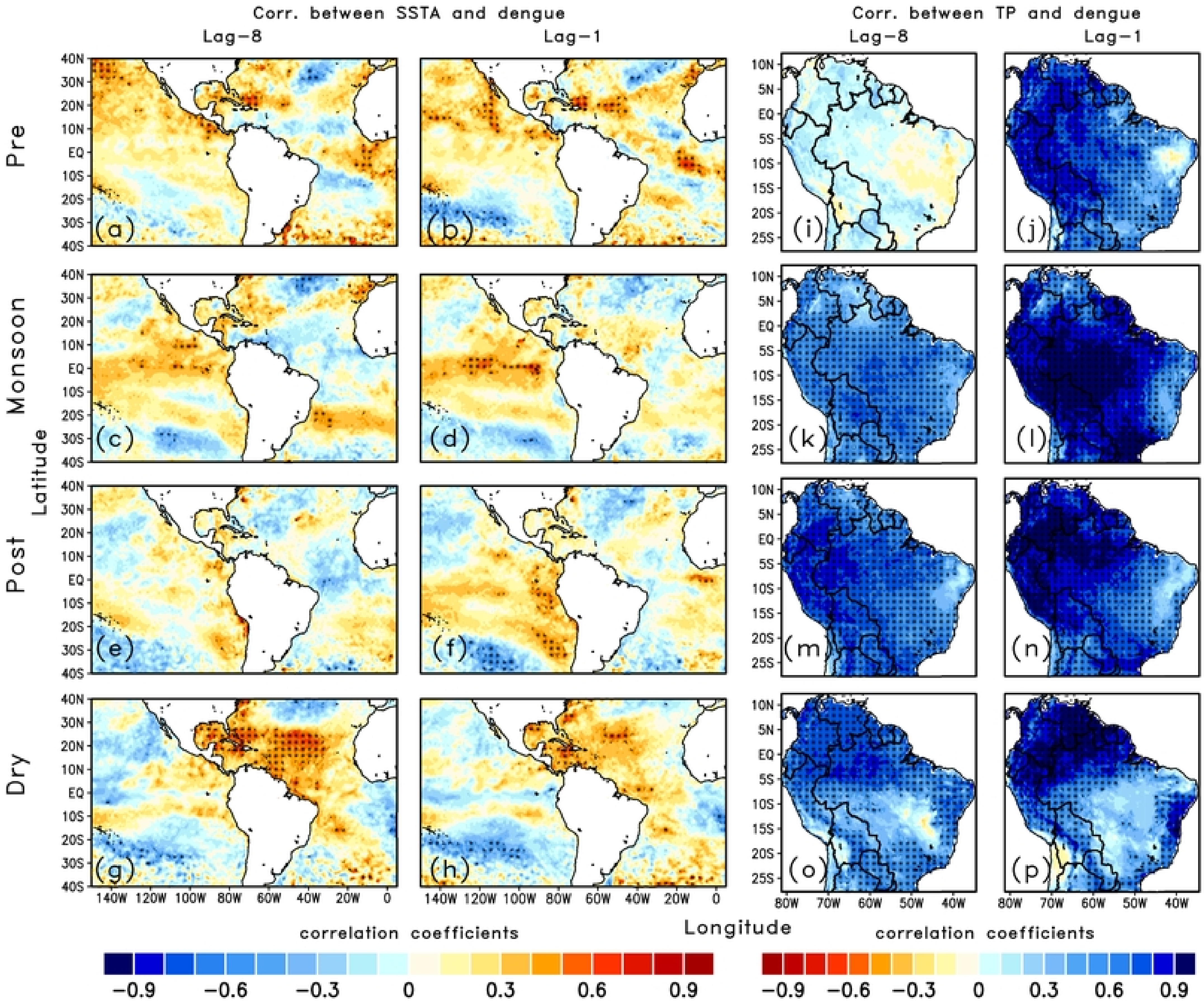

Corr. between SSTA and dengue
Corr. between TP and dengue
Lag-8
Lag-1
Lag-8
Lag-1
Pre
Monsoon
Post
Dry
Latitude
Longitude
(a)
(b)
(c)
(d)
(e)
(f)
(g)
(h)
(i)
(j)
(k)
(l)
(m)
(n)
(o)
(p)
40N
30N
20N
10N
EQ
10S
20S
30S
40S
10N
5N
EQ
5S
10S
15S
20S
25S
140W 120W 100W 80W 60W 40W 20W 0
80W 70W 60W 50W 40W
correlation coefficients
−0.9 −0.6 −0.3 0 0.3 0.6 0.9
correlation coefficients
−0.9 −0.6 −0.3 0 0.3 0.6 0.9

Figure 4

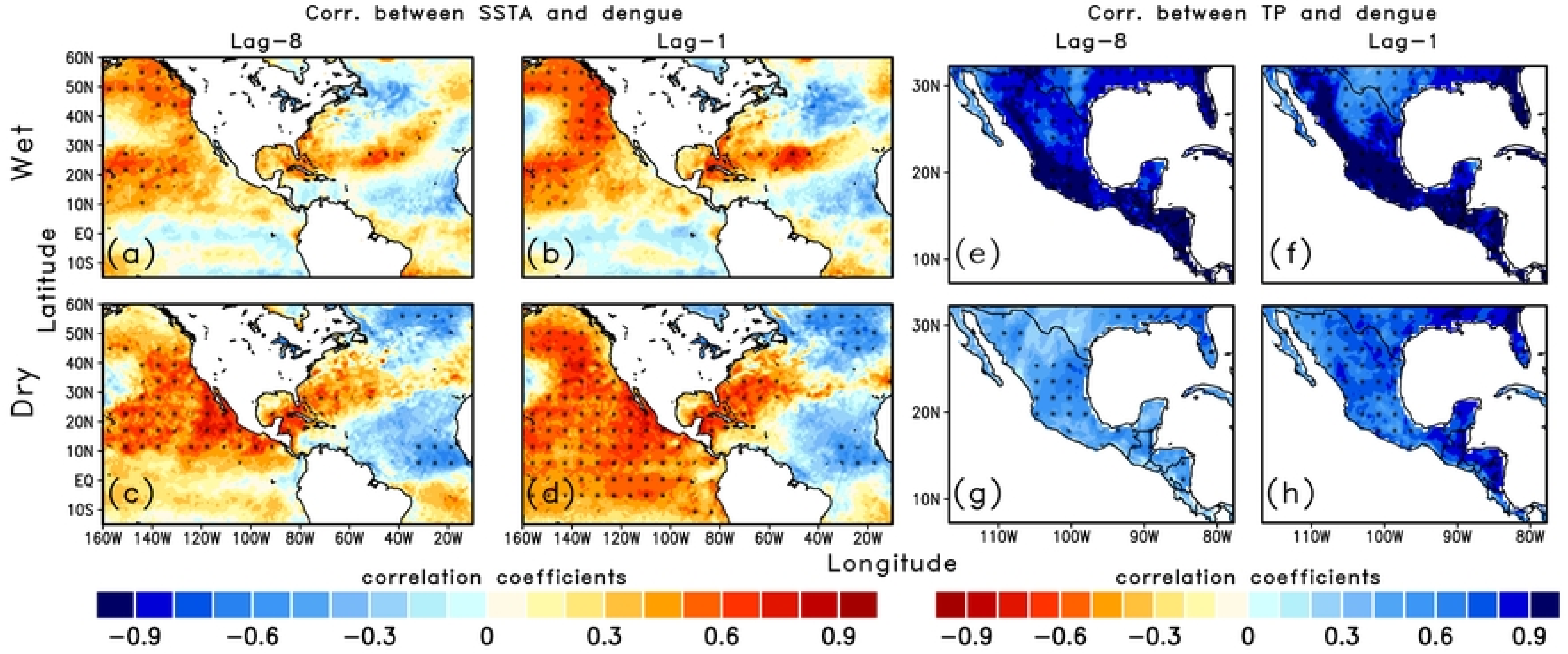
Corr. between SSTA and dengue
Corr. between TP and dengue
Lag-8
Lag-1
Lag-8
Lag-1
Wet
Dry
Latitude
Longitude
(a)
(b)
(c)
(d)
(e)
(f)
(g)
(h)
60N
50N
40N
30N
20N
10N
EQ
10S
160W
140W
120W
100W
80W
60W
40W
20W
110W
100W
90W
80W
correlation coefficients
-0.9
-0.6
-0.3
0
0.3
0.6
0.9

Figure 3

Lag - i: ith weeks before TED
Travel end date (TED)
Lag - 24
Lag - 16
Lag - 8
Lag - 1
Time
$r\overline{SSTA}$, $r\overline{TP}$, $\overline{SSTA}$, $\overline{TPA}$
Day of illness onset

Figure 2

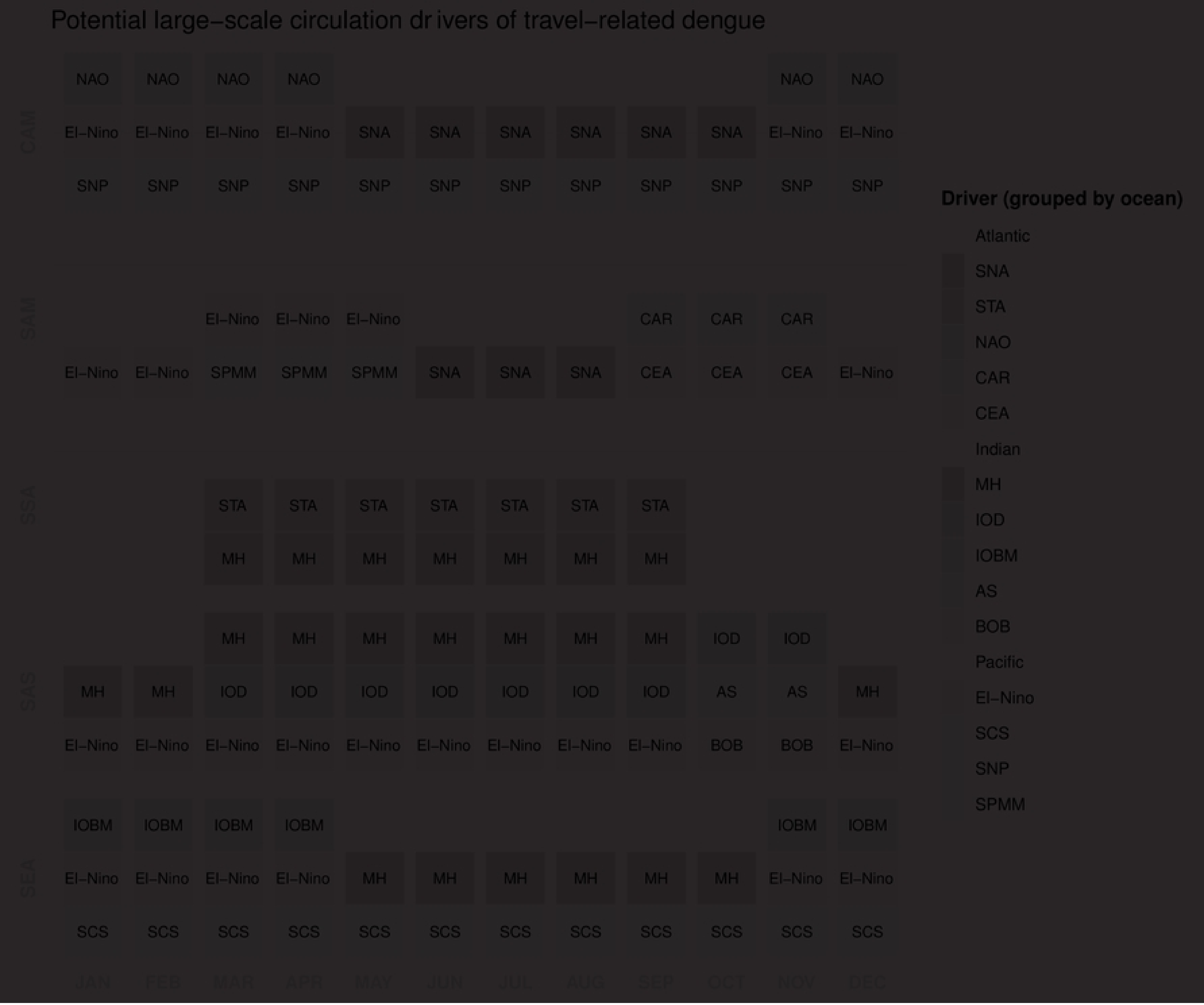

Potential large−scale circulation drivers of travel−related dengue
CAM
SAM
SSA
SAS
SEA
NAO
El−Nino
SNP
SNA
CAR
CEA
SPMM
STA
MH
IOD
AS
BOB
IOBM
SCS
JAN
FEB
MAR
APR
MAY
JUN
JUL
AUG
SEP
OCT
NOV
DEC
Driver (grouped by ocean)
Atlantic
SNA
STA
NAO
CAR
CEA
Indian
MH
IOD
IOBM
AS
BOB
Pacific
El−Nino
SCS
SNP
SPMM

Figure 8